# Experimental Investigation of Thrust Faults

Vahe Gabuchian[1], Ares J. Rosakis[1], Nadia Lapusta[1,2], David Oglesby[3]
[1] Division of Engineering and Applied Science, Caltech [2] Division of Geophysics and Planetary Sciences, Caltech
[3] Department of Earth Sciences, UC Riverside

## Earthquake Visualization Laboratory

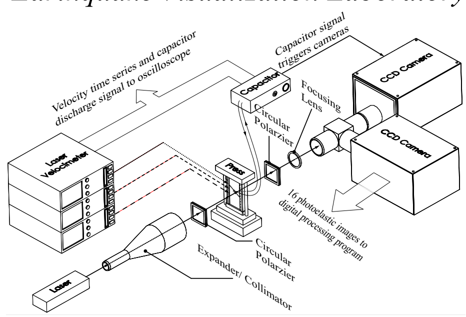


The Earthquake Visualization Laboratory has two unique types of outputs which are used synergistically to study dynamic mode II ruptures with Homalite, a birefringent high density polymer, as the surrogate meterial. A laser source is used to capture 16 digital photoelastic images of the dynamic event with two high speed cameras capable of up to 100 million fps. Three velocimeters can be focused on reflective tapes and measure the surface velocities at those points. Velocimeters and cameras are triggered off the capacitor discharge.

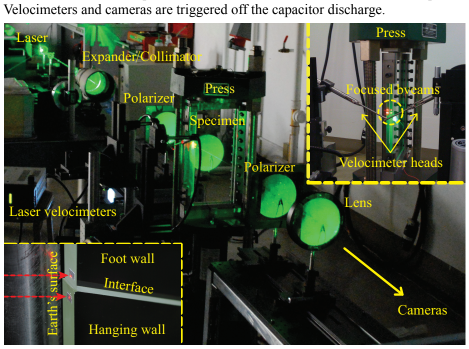


## Initiating simulated thrust fault event

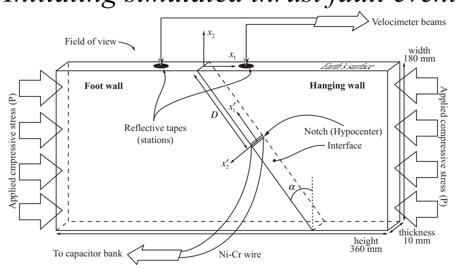


A thin rectangular plate of Homalite has an interface where the simulated hanging and foot walls mate. The interface is carefully and repeatably treated. A notch is machined on the hanging wall half where a wire is placed prior to loading the specimen. The capacitor is discharged across the wire, creating a local pressure increase which initiates the dynamic mode II rupture and triggers the diagnostics. Laser velocimeters record near fault trace ground motions.

## Avoiding reflected waves and buckling

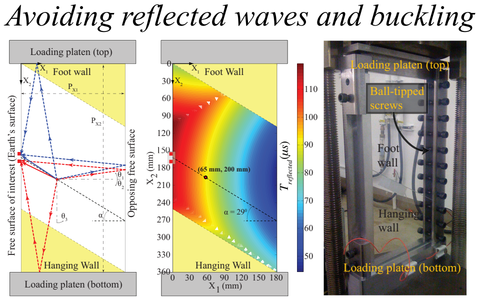


To avoid reflected waves from the top, bottom platens and the opposing free surface, a numerical study of reflected wave arrival times is conducted to avoid reflected waves for roughly 120 μs (it takes the incident S wave 60 μs to reach near fault trace stations). Naturally this requires larger specimen dimensions. Plate width is limited by press width and height by buckling constraints of a larger specimen. A linear array of ball-tipped screws prevents out of plane motion while allowing in-plane motions, increasing the critical buckling load.

## Rupture features and their arrival timing

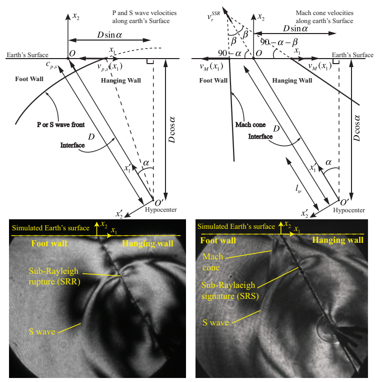


Fringes in photoelastic images represent contours proportional to maximum shear stress, $\tau_{max}$. The left column is a sub-Rayleigh event, the right is supershear. The S wave is visible in both events. The sub-Rayleigh rupture (or the sub-Rayleigh signature in the event where the rupture has transitioned to supershear) is identified by the double-lobe fringe pattern. The Mach cone, a characteristic of a supershear event, has just reached the fault trace. The P wave speed is about twice that of the S wave ($c_p$ = 2.69 mm/μs and $c_s$ = 1.27 mm/μs) and is captured only in early frames. The schematics above are used to generate arrival timing curves for the P wave ($t_p$), S wave ($t_s$), and Mach fronts ($t_M$) as functions of distance from the fault trace, $x_1$.

## Surface breaking thrust fault ground motions

The velocimeters sense long wavelength surface normal motions on the order of 0.25 m/s with the arrival of the P wave, but the surface does not break, as noted by the two black curves moving in unison. The arrival of the S wave moves the stations vertically upward, and is shortly followed by the sub-Rayleigh rupture, which breaks the surface and causes the largest ground shaking. The asymmetry in the ground motion amplitudes is apparent The hanging wall exhibits enhanced ground shaking. Lines emanating from $t_{SRR}$ represent the Rayleigh speed. The spatial attenuation with distance from the fault trace of the SRR signature are studied. Though peak magnitudes are larger in hanging v.s. foot wall, non-dimensional decay rates are nearly identical.

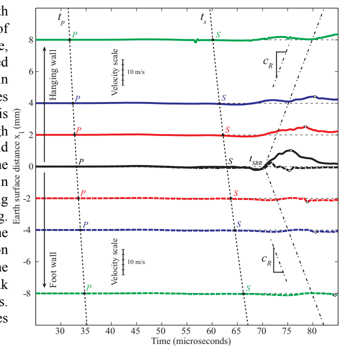


Supershear events are generated by increasing the applied load. The arrival of the Mach fronts to the stations are marked by $t_M$ and cause the largest vertical ground motions. Ground motions are greater on the hanging wall versus the foot wall, similar to the asymmetry in the sub-Rayleigh event. The spatial attenuation of the M peaks are studied. It is expected that the characteristic nature of the Mach fronts will decay its signal at a lower rate than the other features recorded. The ground motions are greater than a sub-Rayleigh event, as expected. The red timing curve $t'_M$ signifies arrivals of Mach fronts emanating from a down-dip traveling supershear rupture. Remnants of the sub-Rayleigh rupture trail behind the S wave.

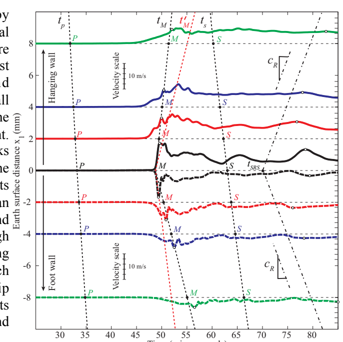


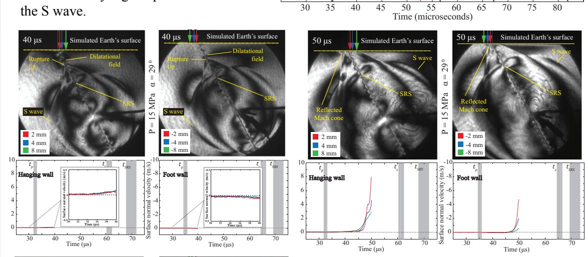


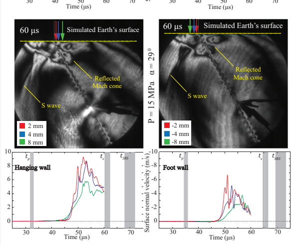


The photoelastic image/trace sequence shows the recently transitioned supershear event, the rupture tip arriving at the fault trace, and the down-dip propagating supershear rupture. Measuring the angle of the down-dip Mach front to the interface and using the Mach-angle relation shows an approximate 17% increase in the reflected versus incident rupture tip speeds. This increase in speed is caused by the different interface condition due to the region being already once processed over by the up-dip rupture and a lower resolved shear stress along the interface due to accumulated slip.

## Signature attenuation study

The peak vertical ground motions associated with the arrivals of the supershear and sub-Rayleigh rupture tips are recorded and plotted against the station's perpendicular distance from the fault trace, $x_1$. As expected, the peak velocities of supershear events are greater than those of a sub-Rayleigh events. The peak velocities in the supershear case occur when the Mach fronts sweep the station while the sub-Rayleigh peak velocities occur with the arrival of the rupture tip. In both supershear and sub-Rayleigh events, the asymmetry in ground motions between the hanging and foot walls is observed, with larger peak magnitudes on the hanging wall. A non-dimensional plot of the data shows that the attenuation rates of the supershear peaks are less than those of the sub-Rayleigh peaks for distances outside $|x_1|$ = 2 mm from the fault trace. Very close to the fault trace ($|x_1|$ < 2 mm) the supershear peak attenuates at a faster rate than the sub-Rayleigh peaks, suggesting that the local effects of the sub-Rayleigh rupture are dominant in the near field while the effects of the supershear rupture influences a larger area, as expected from the characteristic nature of Mach fronts.

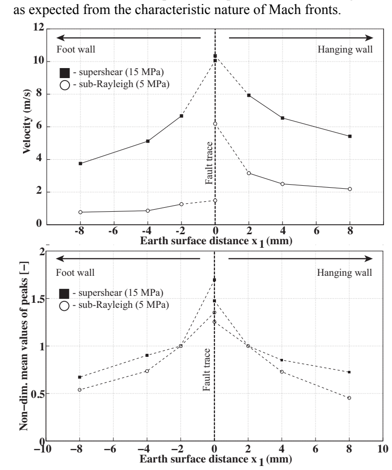


## Blind thrust faults

A heterogeneity is introduced in the interface by covering up a patch of length $l_{patch}$ after polishing the interface and prior to bead blasting. The photoelastic images show two different specimens under a static load of P = 5 MPa roughly 5 minutes before discharging the capacitor bank. The left photoelastic image has no patch and the second has a patch of $l_{patch}$ = 8 mm. The stress concentration is absent in the left image (no patch), and is represented by the fringe concentration in the right. The picture on the right shows the specimen under load with the expanded and collimated green laser light shining through the Homalite. The polished patch near the fault trace shines as it reflects light. This surface heterogeneity will be used to study the differences in ground motions between surface breaking and blind thrust faults.

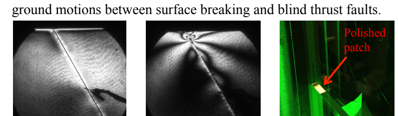


No patch | $l_{patch}$ =8 mm | Reflective patch

## Conclusions and observations

Thrust faults are studied in the laboratory by initiating controlled, repeatable dynamic mode II ruptures along a weak plane (interface) with a thin slab of Homalite as the surrogate material. The lab has two different types of outputs, three temporally resolved point velocity time series (laser velocimeters) focused anywhere along the simulated Earth's surface and 16 spatially resolved photoelastic images of the dynamic event (high-speed cameras up to 100 million fps). Longer clean observation windows are needed to study down-dip phenomenon due to the free surface. Unwanted reflected waves are accounted for by a numerical optimization which determines the optimal specimen geometry and accounts for buckling with the addition of ball-tipped screws in the holder design. Ground motions are larger in supersheaer events versus sub-Rayleigh events, as expected. The hanging wall plate exhibits greater ground motions than the foot wall in both supershear and sub-Rayleigh events. The Mach fronts emanating from the discovered down-dip propagating rupture have clear signatures in the ground motion traces. The Mach front signatures attenuate with distance at a slower rate v.s. the sub-Rayleigh rupture peaks, as expected from the characteristic nature of Mach fronts. Near-fault ground motions will further be studied by introducing surface heterogeneities (polished patch) to see the ground motion differences between surface breaking and blind thrust faults.